Peptide hydrolysis by metal-(oxa)cyclen complexes: Revisiting the mechanism and assessing ligand effects

Gantulga Norjmaa,[†] Albert Solé-Daura, Maria Besora, Josep M. Ricart, and Jorge J. Carbó*

Department de Química Física i Inorgànica, Universitat Rovira i Virgili, Marcel·lí Domingo 1, 43007 Tarragona, Spain.

ABSTRACT: The mechanism responsible for the peptide bond hydrolysis by Co(III) and Cu(II) complexes with (oxa)cyclen ligands has been revisited by means of computational tools. We propose that the mechanism starts by substrate coordination and an outer-sphere attack to amide carbon of a solvent water molecule assisted by the metal-hydroxo moiety as a general base, which occurs through six-membered ring transition states. This new mechanism represents a more likely scenario than the previously proposed mechanisms that involved an inner-sphere nucleophilic attack through more strained four-membered rings transition states. The corresponding computed overall free-energy barrier of 25.2 kcal mol^{-1} for the hydrolysis of the peptide bond in Phe—Ala by Co(III)-oxacyclen catalyst (**1**) is consistent with the experimental values obtained from rate constants. Also, we assessed the influence of the nature of the ligand throughout a systematic replacement of N by O atoms in the (oxa)cyclen ligand. Increasing the number of coordinating oxygen atoms accelerates the reaction by increasing the Lewis acidity of the metal ion. On the other hand, the higher reactivity observed for Cu(II)-oxacyclen catalyst respect to the analogous Co(III) complex can be attributed to the larger Brönsted basicity of the Cu(II)-hydroxo ligand. Ultimately, the detailed understanding of ligand and metal nature effects allowed us to identify the double role of the metal-hydroxo complexes as Lewis acids and Brönsted bases and to rationalize the observed reactivity trends.

INTRODUCTION

The selective hydrolysis of highly kinetically inert peptide bonds in biological systems represents an important process within the fields of biochemistry and biotechnology due to its potential application in proteomics,[1] protein sequencing,[1,2] foot printing,[3] and engineering,[4] or the design of new catalytic drugs capable to bind and inhibit pathogenic proteins.[5] Natural hydrolytic enzymes, also called proteases or peptidases can efficiently speed up this chemical reaction, although they are usually expensive and provide poor selectivity. In addition, their biological nature only allows them to operate in a narrow range of temperature and pH. Aiming to overcome these issues, the development of artificial metalloproteases has been largely explored in the last decades. Most of the proposed hydrolytic agents consist in transition metal (TM) complexes based on Co, Cu, Zn, Pd, Pt, Zr, Ni, Mo, Mn, or Fe as hydrolytically active centres.[6]

Specifically, Co(III)- and Cu(II)-based complexes with tetradentate 1,4,7,10-tetraazacyclododecane (cyclen) or 1-oxa-4,7,10-triazacyclododecane (oxacyclen) ligands have shown the ability to hydrolyze selectively a wide range of biological molecules such as lysozyme, myoglobin, albumin, globulin, amyloid-β (Aβ) peptide or human islet amyloid peptide (h-IAPP).[7-26] Importantly, the cyclen family of ligands can incorporate an organic alkyl or aryl pendant that induces an enzyme-like recognition of the catalyst by the biological system, in such a way that the hydrolysis process becomes highly selective. This approach has been successfully applied to hydrolyze Aβ oligopeptides selectively at peptide bonds between Phe20–Ala21 and Ala21–Glu22,[12,20] making metal-cyclen complexes highly attractive as a novel family of drugs for Alzheimer's disease, which is presumably caused by the formation of misfolded aggregates of Aβ oligomers.[27] Nevertheless, although their hydrolytic activity has been extensively studied experimentally, the mechanism governing the hydrolysis process at molecular level is still not fully understood.

Several mechanisms for the peptide hydrolysis assisted by TM complexes have been proposed in the literature.[28-42] Most of them involve the initial coordination of the amide oxygen of the peptide bond to the TM center that acts as a Lewis acid, activating the amide carbon towards a nucleophilic attack. However, they differ from each other in the way in which this nucleophilic attack occurs. Scheme 1 compiles the main mechanistic proposals for the nucleophilic attack step reported in previous computational works, classified on the basis of their inner- or outer-sphere nature. The proposed inner-sphere mechanisms include the direct attack of either a hydroxo (*i* and *ii*) or an aqua ligand (*iii*-*v*) bound to the metal, which can be assisted by a Brönsted base capable of abstracting a proton from the attacking group increasing its nucleophilicity. Among them, the carboxylate group of a residue nearby (*iv*), the amide oxygen (*v*) or nitrogen (*ii* and *iii*) have been considered to act as a general base. The outer-sphere attack of an external water molecule from the solvent has been analyzed as assisted by the amide N (*vi*), by the C-terminal carboxylate group in the hydrolysis of dipeptides (*vii*), or by the metal-hydroxo moiety (*viii*, *this work*).

Scheme 1. Compilation of the computationally studied mechanisms for the peptide bond hydrolysis catalyzed by artificial metalloproteases. Nucleophilic groups are highlighted in red and those acting as a general base in blue.

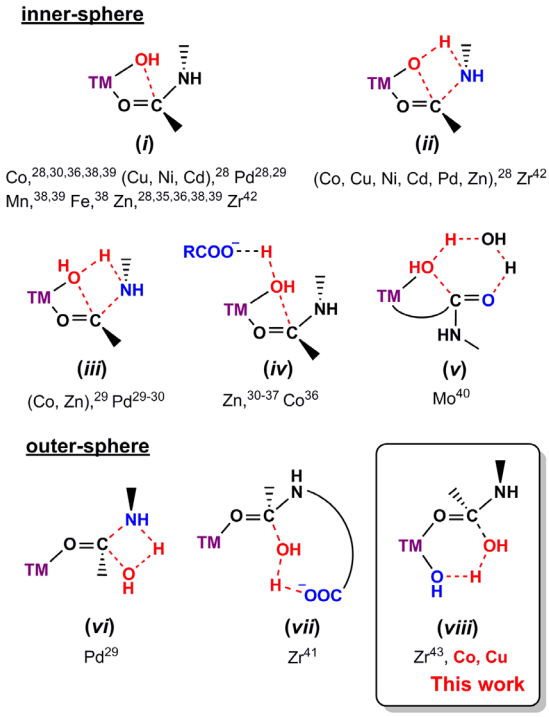

Previous computational studies on monometallic hydroxo complexes,[28-40] including Co- and Cu-(oxa)cyclen complexes,[28] have assumed that the nucleophilic hydroxo ligand attacks directly to the electrophilic, carbonyl carbon. However, we noticed that for first row transition-metals this process involves an unfavorable four-membered ring transition state (Scheme 1, *i-iv*), which, in the case of Co(III)- and Cu(II)-(oxa)cyclen complexes, resulted in a high, computed energy barrier for the hydrolysis of the Phe—Ala dipeptide bond, ca. 40 kcal mol^{-1}.[28] This suggests that hydroxo group could play a different role acting as a basic center to activate the nucleophilic attack of an external water molecule via a more favorable six-membered ring transition state (see Scheme 1). This mechanism has been very recently proposed to be competitive for a second-row transition-metal complex such as the Zr-substituted polyoxometalate.[43] Also recently, Lim and coworkers have performed detailed mechanistic investigations (experimental and computational) on the anti-amyloidogenic activity of closely related Co(II)- and Cu(II)-(tetra-N-methylated cyclam) complexes, concluding that the inhibition activity can be directly related to the hydrolytic cleavage of Aβ peptide bonds.[44] These studies suggested the participation of metal-hydroxo groups; however the extent or degree to which it participates in the amide activation is not clear.[44] Following our interest in the computational modelling of artificial proteases,[45] herein we revisit the previously proposed mechanism[28] for peptide hydrolysis of the Phe—Ala dipeptide by the Co(III)-oxacyclen (**1**, depicted in Figure 1), -cyclen (**1b**) and Cu(II)-oxacyclen complexes (**1**^{Cu}), exploring whether the hydroxo ligand acts as Brönsted base activating an external water for the nucleophilic attack (highlighted in Scheme 1). The new mechanistic proposal allows reproducing and rationalizing the observed reactivity trend as a function of the ligand type and of the metal nature, **1**^{Cu} ≥ **1** > **1b**, and then, to assess the effect of additional ligand modifications.

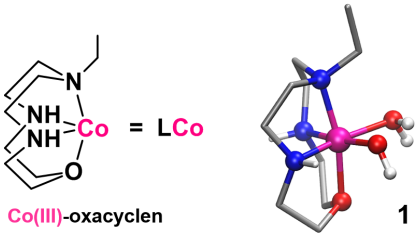

Figure 1. Schematic and ball-and-stick representation of the Co(III)-oxacyclen [N_3O_1] complex **1**, used as artificial metalloprotease. Color code: Co (magenta), C (gray), O (red), N (blue), H (white). C-bonded H atoms are omitted for clarity.

RESULTS AND DISCUSSION

Mechanism for peptide hydrolysis by cobalt-oxacyclen compounds.

To study the feasibility of our mechanistic proposal, we initially reproduced those found in the literature for the peptide hydrolysis by metal-(oxa)cyclen compounds. To do so, we selected the Co(III)-oxacyclen complex **1** as catalyst (Figure 1), employed in previous studies.[28] This complex consists in a 1-oxa-7-ethyl-4,7,10-triazacyclododecane ring coordinated to the Co(III) center in a tetradentate fashion in a syn-anti conformation of the chelating NH groups in positions 4 and 10. Other conformations were computed to be energetically accessible, although the ligand conformation was found to have a minor impact in the reactivity (<3 kcal mol^{-1} range in free-energy barriers). The alkyl pendant used experimentally to induce selectivity was modelled as an ethyl group bonded to the nitrogen in position 7, and the N- and C-terminus fragments of the Phe20—Ala21 dipeptide were capped with a –H and a –Me groups, respectively.

Figure 2 compares the free-energy profile associated to the novel mechanism viii (see Scheme 1) with that of the previously proposed inner-sphere pathway. The initial coordination of the amide oxygen to the Co center to replace an aqua ligand from species **1** is endothermic by 5.8 kcal mol^{-1} and yields the hydrolytically active species **2**, in which the amide carbon is activated by the Lewis-acid effect of the metal center. From this species, the inner-sphere nucleophilic attack of the hydroxo ligand can take place through a four-membered ring TS structure (**TS$_{2\text{-}3}$**, shown in Figure 2) overcoming a high, but still affordable, free-energy barrier of 29.4 kcal mol^{-1} from the reactants. This generates the tetrahedral intermediate **3** (Figure S1), which corresponds to a rather shallow minimum located at 29.0 kcal mol^{-1} above the reactants. It was proposed that **3** can evolve to products through another four-membered ring TS (**TS$_{3\text{-}P}$**, represented in Figure 3) that implies the concerted C—N bond cleavage and proton transfer from the hydroxyl group to the leaving amine nitrogen.[28] According to our calculations, this process would need to overcome a prohibitively high, overall free-energy barrier of 45.0 kcal mol^{-1}, as shown in Figure 2. This value is similar to previously reported values of ca. 40 kcal mol^{-1},[28] which do not account for the endothermicity of the peptide coordination (**1** → **2**). The highly unstable character of **TS$_{3\text{-}P}$** was ascribed to the stain induced by the two condensed four-membered rings. Thus, we considered this pathway inaccessible even at the experimental temperature of 50 ºC.

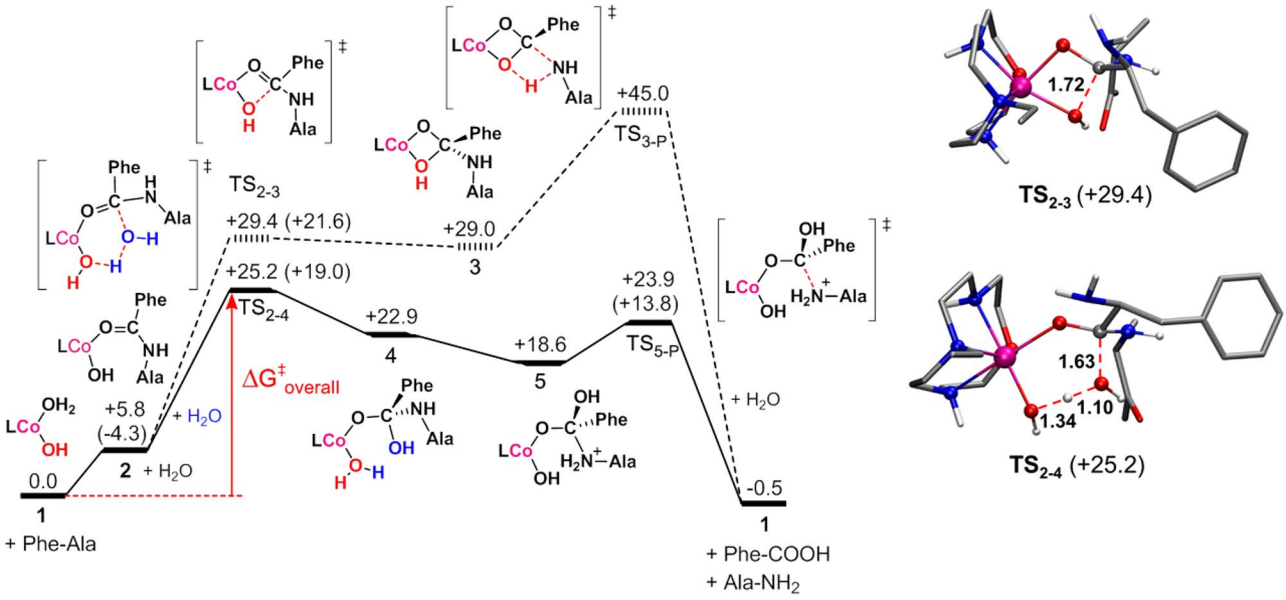

Figure 2. Gibbs free-energy (kcal mol^{-1}) profile for the peptide bond hydrolysis in Phe–Ala catalyzed by the Co(III)-oxacyclen complex **1**. Solid lines represent the herein proposed outer-sphere mechanism, whereas the more energy-demanding inner-sphere is represented in dashed lines. Values in parenthesis were computed at B3LYP-D3/TZVP level for comparison. The red arrow highlights the rate-determining step. Structures on the right panels correspond to the optimized geometries for **TS$_{2\text{-}3}$** and **TS$_{2\text{-}4}$**, associated to the nucleophilic attack step in the inner- and the outer-sphere mechanisms, respectively. Main distances in Å. C-bonded H atoms are omitted for clarity.

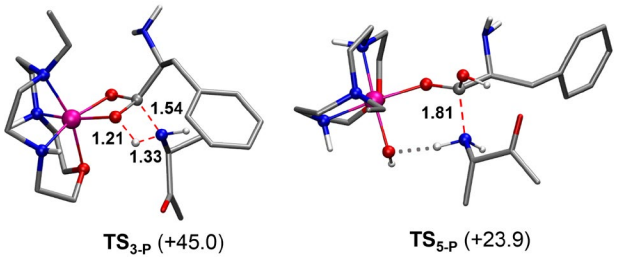

Figure 3. B3LYP-optimized geometries for the transition states (**TS$_{3\text{-}P}$** and **TS$_{5\text{-}P}$**) for the C—N bond cleavage in the hydrolysis of Phe—Ala bond by the Co(III)-oxacyclen catalyst **1**. Main distances shown in Å and relative energies to the reactants in kcal mol^{-1}. C-bonded H atoms are omitted for clarity.

Alternatively, the outer-sphere nucleophilic attack of an external water molecule from the solvent, assisted by the Co—OH moiety acting as a Brönsted base occurs through a less strained, six-membered ring transition state (**TS$_{2\text{-}4}$**, displayed in Figure 2). This process involves a lower free-energy barrier of 25.2 (from **1** to **TS$_{2\text{-}4}$**) that can be readily overcome at the experimental conditions. Thus in this case, we can conclude that the outer-sphere mechanism is more favorable than the inner-sphere one. The resulting tetrahedral intermediate **4** (Figure S1) lies 22.9 kcal mol^{-1} above the reactants, being ~4 kcal mol^{-1} more stable than the intermediate resulting from the inner-sphere nucleophilic attack **3**. The intermediate **4** rapidly evolves to the more stable species **5** (4.3 kcal mol^{-1} below in energy) after a bond rotation about the single (Co)O—C bond that induces a proton transfer from the aqua ligand to the amide nitrogen. The proton transfer step was found to be barrierless or to occur through a very smooth barrier, since all the attempts of characterizing the conformational isomer of **4** generated via bond rotation led to species **5**. Nevertheless, we could estimate a barrier of < 1 kcal mol^{-1} based on electronic energies obtained by including one explicit solvent molecule in the model that stabilizes the strongly polarized species involved in this process (see Scheme S1). Upon protonating the amide nitrogen, the C—N bond is weakened as reflected in the distance elongation from 1.45 Å in **4** to 1.60 Å in **5**. This permits the C—N bond cleavage through a rather smooth free-energy barrier of 5.3 kcal mol^{-1} (**TS$_{5\text{-}P}$** in Figure 3). This final step yields the hydrolysis products, and upon a coordination of a water molecule to Co, the catalytic complex **1** is recovered to close the catalytic cycle.

The overall peptide hydrolysis process is computed to be exergonic by 0.5 kcal mol^{-1} as shown in Figure 2. The highest-energy species in the outer-sphere mechanism (solid lines in Figure 2) is the transition state for the water nucleophilic attack to amide carbon (**TS$_{2\text{-}4}$**), resulting in a computed overall free-energy barrier of 25.2 kcal mol^{-1}. Importantly, this value is significantly closer to the experimental rate constants, from which we can estimate free-energy barriers of ca. 25-26 kcal mol^{-1} (see Table S2),[16,19] than that from previous proposed mechanism (~40 kcal mol^{-1}).[28] To check our methodology, we have re-evaluated the initial steps of the mechanism using a larger basis set and introducing dispersion corrections to DFT method (B3LYP-D3/TZVP level, see Computational Details). At this level, the computed free energy barrier for water attack through (**TS$_{2\text{-}4}$**) is 23.3 kcal mol^{-1}, also close to experimental values. In addition, **TS$_{2\text{-}4}$** is also lower than the transition state for the inner-sphere mechanism (**TS$_{2\text{-}3}$**) and higher than the the transition state for C-N cleavage (**TS$_{5\text{-}P}$**) by 2.6 and 5.6 kcal mol^{-1}, respectively (see Table S1). Moreover, depending on the corrections to the obtained Gibbs free energies (see Computational Details), the computed overall barrier varies from 23.3 to 25.0 kcal mol^{-1}, getting closer to experiments. We note that dispersion corrections enhance the non-bonding interaction between the catalyst and the dipeptide substrate yielding to a slightly exergonic coordination of the dipeptide to form intermediate **2**, which becomes resting-state of the process. Nevertheless, we have not been able to find any experimental

evidence for the formation of such a metal-peptide adduct. This suggests that dispersion corrections could overstabilize the catalyst-substrate interactions, but they are present in the reactant and the transition state, and consequently do not affect the energy barrier.

In summary, the activity of the reaction is governed the external water nucleophilic attack to the amide carbon. However, the transition state for the C—N cleavage (**$TS_{5\text{-}P}$**) is close in energy to **$TS_{2\text{-}4}$**, and therefore, variations in the ligand or in the metal nature could switch the rate-determining transition state. Moreover, the inner-sphere mechanism involving four-membered ring transition states such as **$TS_{2\text{-}3}$** structure could be significantly stabilized by second row transition metal elements.[46] In fact, Prabhakar et al. have recently found low free-energy barriers (<15 kcal mol^{-1}) for metal-hydroxo nucleophile attack to the amide carbonyl carbon in second-row Zr(IV) complexes bearing diaza-18-crown-6 ligands.[42]

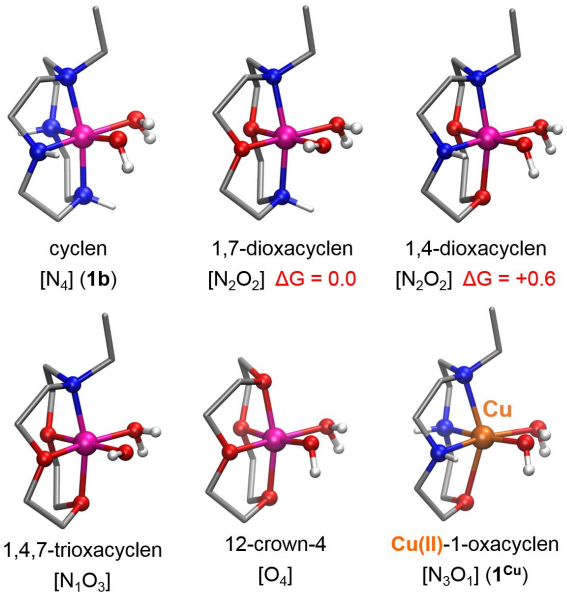

Figure 4. Ball-and-stick representation of the DFT-optimized structures for the Co(III)-based cyclen [N_4] (**1b**), 1,7- and 1,10-dioxacyclen [N_2O_2], 1,4,10-trioxacyclen [N_1O_3] and 12-crown-4 [O_4] and the Cu(II)-based 1-oxacyclen [N_3O_1] (**1^{Cu}**) catalysts. Relative Gibbs free energies for two isomers of the Co-dioxacyclen compound are given in kcal mol^{-1}.

Influence of the ligand and the metal nature on the activity

Several kinetic studies on the peptide hydrolysis by metal-cyclen complexes suggested that the reaction rate is sensitive to the features of the ligand and the nature of the TM ion. In general, cobalt complexes with oxacyclen [N_3O_1] ligands (**1** in Figure 1) perform better than Co-cyclen [N_4] ones (**1b** in Figure 4), attaining the hydrolysis of the substrate up to ten times faster.[16] In addition, Suh and co-workers showed that Cu(II)-oxacyclen complexes can exhibit greater hydrolytic activity than their Co(III)-based analogues,[10,13,17,19] although they are less popular for in vivo applications because Cu(II) ions can be more easily released from the catalyst structure to the medium in a living body.[8] The proposed metal-hydroxo base-assisted mechanism provides a new platform to evaluate the influence of the ligand and the metal nature on the peptide hydrolysis activity by comparing different catalytic structures.

Table 1. Influence of the Nature of the Ligand in the Hydrolysis of Phe—Ala Peptide Bond by Co(III) Complexes.[a]

Ligand (compound)	Coord atoms	$d_{TM\text{-}OC}$	$\pi^*_{C=O}$ (energy)	$\Delta G^{\ddagger}$ (**1**→**$TS_{2\text{-}4}$**)
cyclen (**1b**)	N_4	2.13	+14.4	28.5
1-oxacyclen (**1**)	N_3O_1	2.04	+14.0	25.2
1,7-dioxacyclen	N_2O_2	2.05	+14.3	25.9
1,4-dioxacyclen[b]	N_2O_2	2.03	+13.9	23.9
1,4,7-trioxacyclen	N_1O_3	1.94	+13.4	19.5
12-crown-4	O_4	1.92	+12.9	15.2

[a] Distances in Å, energies of Natural Bond Orbitals in eV and Gibbs free-energy barriers in kcal mol^{-1}. [b] The Co-1,4-dioxacyclen complex in which the oxygen of the ligand and the hydroxo ligand are in cis conformation is > 5 kcal mol^{-1} less stable and therefore, it was not considered.

First, we analyzed the influence of the ligand by comparing the reactivity of **1** towards the Phe—Ala peptide bond hydrolysis with that of the experimentally tested Co-cyclen **1b**, which does not contain any oxygen in the structure of the ligand. Then, we explored other Co complexes containing different number of coordinating oxygen atoms in the ligand scaffold. Using the ligand of complex **1** as reference, the N atoms were systematically replaced by O atoms, evaluating the free-energy barriers for the rate-determining process (from the reactants to **$TS_{2\text{-}4}$**). The studied catalytic species are displayed in Figure 4 and Table 1 compiles the free-energy barriers obtained for the most stable isomer of each of the ligands. Importantly, we observed a decrease in the overall free-energy barrier when moving from the Co-cyclen complex **1b** to the Co-oxacyclen **1** ($\Delta G^{\ddagger}$(**1**→**$TS_{2\text{-}4}$**) of 28.5 and 25.2 kcal mol^{-1}, respectively). Experimentally, **1** can promote the hydrolysis of peptide bonds up to the ten-fold faster than **1b**,[16] which corresponds to a $\Delta\Delta G^{\ddagger}$ of 1.5 kcal mol^{-1}. Thus, the computed energy difference of ca. 3 kcal mol^{-1} is not only in qualitative but in quantitative agreement with the experimental data, further validating the new mechanistic proposal.

Table 1 reveals a general trend upon systematic replacement of coordinating amino groups by oxygen atoms. Roughly, the higher is the number of coordinating oxygen atoms in the ligand, the lower the free-energy barrier and consequently, the faster the hydrolysis. Comparing 1,7- and 1,4-dioxacyclen ligands (Figure 4), we also found that the coordination position of the oxygen atoms has also an influence on the hydrolysis activity. Thus, the coordination of an oxygen atom trans to the aqua ligand, which has to be replaced by the amide carbonyl group, disfavors peptide hydrolysis. As previously postulated by Kim et al. on the basis of the experimental, catalytic activity of **1** and **1b**,[16] this reactivity trend can be ascribed to the decreased basicity of the ligand upon incorporating oxygen atoms, which increases the Lewis acidity of the metal and in turn, favors the activation of the amide carbon towards a nucleophilic attack. In agreement with this hypothesis, we found a clear correlation (see Table 1) between the overall free-energy barriers and the distance between the cobalt ion and the amide oxygen in Co-dipeptide complex (analogous to species **2** in Figure 2). The distance decreases with the number of coordinating oxygen atoms as a consequence of the larger Lewis acidity of Co ion resulting in lower free-energy barriers. Accordingly, the energy of the $\pi^*_{C=O}$ molecular orbital that receives the nucleophilic attack of water molecule decreases by increasing the number of O atoms in the cryptand (going down the 4th column in Table 1). These trends are also observed for the two dioxocyclen isomers differing on the geometric position of the oxygen donor atoms. The less reactive Co-1,7-dioxacyclen complex has larger C-O(=C) distances and higher energy-lying $\pi^*_{C=O}$ molecular orbital than Co-oxacyclen (**1**) and Co-1,4-doxacyclen complexes (see Table 1). There are not experimental evidences corroborating the computational results for the hydrolysis of Aβ oligomers catalyzed by di-, trioxacyclen or 12-crown-4. However, this reactivity trend was observed for the cleavage of DNA using Cu(II) complexes,[47] suggesting that indeed, an increasing content of oxygen in oxacyclen ligands would facilitate the activation of highly kinetically inert peptide bonds by TM complexes.

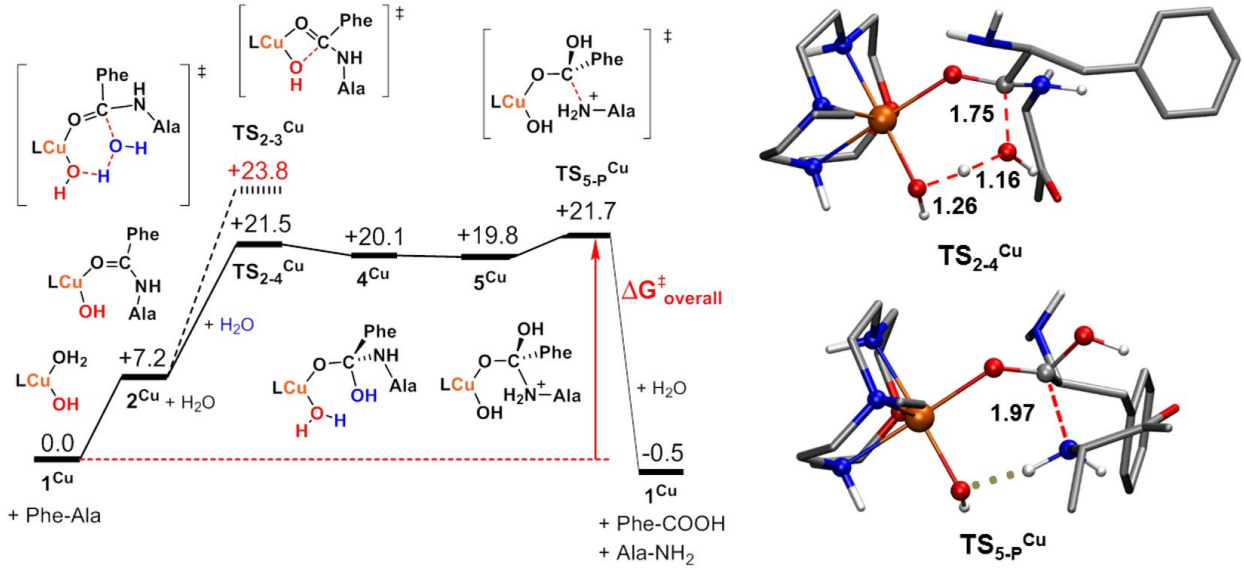

Figure 5. Gibbs free-energy profile (kcal mol^{-1}) for the peptide bond hydrolysis in Phe–Ala catalyzed by the Cu(II)-oxacyclen complex $\mathbf{1}^{Cu}$. Solid and dashed lines represent the outer- and the inner-sphere mechanisms, respectively. The red arrow highlights the rate-determining step. Structures on the right panels correspond to the optimized geometries for $\mathbf{TS_{2\text{-}4}}^{Cu}$ and $\mathbf{TS_{5\text{-}P}}^{Cu}$. Main distances shown in Å. C-bonded H atoms are omitted for clarity.

Next, we evaluated the influence of the nature of the metal by comparing the behavior of cobalt complex **1** with the analogous Cu(II)-oxacyclen catalyst $\mathbf{1}^{Cu}$, both coordinating the same 1-oxa-7-ethyl-4,7,10-triazacyclododecane ligand (Figure 4 and 5). Also, we computed the key mechanistic steps for another geometric isomer of the ligand, the syn-1-oxa-4-ethyl-4,7,10-triazacyclododecane, resulting in complex $\mathbf{1}^{Cu'}$ (Figure S3). Note that previous computational studies have considered the Cu complex $\mathbf{1}^{Cu'}$, which is the most stable isomer,[28] but as we will discuss below it is not the most reactive. Thus, we will focus the discussion on complex $\mathbf{1}^{Cu}$ since the differences with cobalt complex **1** can be only attributed to the nature of the metal and not to the geometry of the ligand. Figure 5 shows the free-energy profile for the Phe—Ala hydrolysis by $\mathbf{1}^{Cu}$ and the geometries of key species. Although the coordination of the dipeptide to the Cu(II) center is somewhat more endergonic than for Co(III) (+7.2 vs +5.8 kcal mol^{-1}), the overall free-energy barrier for the outer-sphere nucleophilic attack in Cu(II) complex ($\Delta G^{\ddagger}(\mathbf{1}^{Cu} \rightarrow \mathbf{TS_{2\text{-}4}}^{Cu})$ = 21.5 kcal mol^{-1}) is appreciably lower than that found for Co (25.2 kcal mol^{-1}). As a consequence, the transition state for C—N cleavage ($\mathbf{TS_{5\text{-}P}}$) becomes slightly higher in energy (21.7 kcal mol^{-1}), determining the overall free-energy barrier of the process (see Figure 5). Also for Cu complex, the transition state for the inner-sphere attack of the Cu-hydroxo moiety to the amide carbon of the peptide ($\mathbf{TS_{2\text{-}3}}^{Cu}$) is higher in energy than the outer-sphere attack ($\mathbf{TS_{2\text{-}4}}^{Cu}$), by 2.3 kcal mol^{-1} in this case (Figure 5).

In going from the cobalt **1** to the copper $\mathbf{1}^{Cu}$ complex, we computed an appreciable reduction of the overall free-energy barrier of 3.5 kcal mol^{-1}, indicating that Cu(II) is more reactive than Co(III) metal. This trend is clearly observed when comparing experimental rate constants of Co(III)- and Cu(II)-

cyclen complexes,[10,15,16] for which the estimated energy difference is ~2 kcal mol^{-1} (see Table S2). For oxacyclen complexes the energy difference is smaller (Table S2),[10,13,17,19] but comparison between them is more difficult because Co and Cu complexes could be active in different structural isomers. In fact, we characterized another structural isomer $\mathbf{1}^{\mathbf{Cu'}}$ (depicted in Figure S3) which lies 1.5 kcal mol^{-1} below $\mathbf{1}^{\mathbf{Cu}}$. Interestingly, $\mathbf{1}^{\mathbf{Cu'}}$ catalyst shows a higher overall barrier ($\Delta G^{\ddagger}(\mathbf{1}^{\mathbf{Cu'}} \rightarrow \mathbf{TS_{2\text{-}4}}^{\mathbf{Cu'}})$ = 24.6 kcal mol^{-1}) than $\mathbf{1}^{\mathbf{Cu}}$, slightly lower than that calculated for Co catalyst **1** (25.2 kcal mol^{-1}). As shown in Figure S4, the oxygen atom of the ligand is partially decoordinated from the Cu center during the nucleophilic attack (Cu—O distance elongation from 2.56 Å in $\mathbf{2}^{\mathbf{Cu'}}$ to 2.71 Å in $\mathbf{TS_{2\text{-}4}}^{\mathbf{Cu'}}$), yielding a distorted trigonal bipyramid geometry around the Cu(II) in the transition state. In fact, the high lability of Cu-bonded ligands has been observed experimentally.[8]

To further investigate the origin of the different catalytic activity of Co- and Cu-containing oxacyclen complexes, we compared the electronic properties of the catalyst-substrate coordination complexes **2** and $\mathbf{2}^{\mathbf{Cu}}$ (Table 1 and 2). Interestingly, although the more electron-rich Cu(II) center is a weaker Lewis acid than Co(III),[48] it displays a lower overall barrier. For $\mathbf{2}^{\mathbf{Cu}}$, this trend is manifested in the lower polarization and stabilization of the $\pi^*_{C=O}$ antibonding orbital of the coordinated amide carbonyl group that receives the nucleophilic attack ($E(\pi^*_{C=O})$ = +15.3 and +14.0 eV for $\mathbf{2}^{\mathbf{Cu}}$ and **2**, respectively). Thus, the higher reactivity of copper complexes has to be explained by the stronger basicity of the Cu(II)—OH moiety that abstracts a proton from an external water molecule during the nucleophilic attack. Accordantly, the NPA atomic charge supported by the O atom of the hydroxo group is more negative in $\mathbf{2}^{\mathbf{Cu}}$ (−1.08 a.u.) than in **2** (−0.91 a.u.), what is fully consistent with the experimentally determined pK_a values for the respective TM-aqua complexes of 3.3 for Co(III)[16] and 8.7 for Cu(II).[17] The electronic features of $\mathbf{2}^{\mathbf{Cu'}}$ isomer are similar to those of $\mathbf{2}^{\mathbf{Cu}}$ but slightly less pronounced in comparison with the cobalt complex **2** (see Table 2). Overall, this analysis shows that Co- and Cu-hydroxo complexes have an ambiphilic behavior in the catalysis of peptide hydrolysis acting both as Lewis acids and Brönsted bases. For these complexes the Brönsted basicity of the hydroxo ligand controls their relative reactivity.

Table 2. Geometric and Electronic Properties and Reactivity towards the Phe—Ala Peptide Bond of Two Different Isomers ($\mathbf{2}^{\mathbf{Cu}}$ and $\mathbf{2}^{\mathbf{Cu'}}$) of the Cu(II)-Oxacyclen Catalyst.[a]

species	$d_{TM\text{-}OC}$	$\pi^*_{C=O}$ (energy)	$q_{O,hydroxo}$	$\Delta G^{\ddagger}_{overall}$
$\mathbf{2}^{\mathbf{Cu}}$	2.19	15.3	-1.08	21.7
$\mathbf{2}^{\mathbf{Cu'}}$	2.19	15.0	-1.07	24.6

[a] Distances in Å, Gibbs free energies in kcal mol^{-1}; energies of Natural Bond Orbitals in eV and atomic charges derived from NPA analysis in a.u.

CONCLUSIONS

Herein, we propose a new mechanism for the hydrolysis of peptide bonds catalyzed by Co(III) and Cu(II)-(oxa)cylen artificial metalloproteases, based on DFT calculations, that consists of four main steps: 1) coordination of the peptide substrate to the metal atom replacing one aqua ligand; 2) outer-sphere nucleophilic attack of a solvent water molecule to the amide carbon assisted by the metal center as a Lewis acid in addition to the TM–OH moiety acting as a Brönsted base; 3) proton transfer to the amide nitrogen atom from the TM–OH_2 moiety; 4) cleavage of the C—N bond to yield the products. The outer-sphere nucleophilic attack involves a six-membered ring transition-state structure, which is more favored than the previously proposed inner-sphere nucleophilic attack of the hydroxo ligand through a strained, four-membered ring structure. The new value for the computed overall free energy barrier for the peptide hydrolysis in Phe—Ala catalyzed by the Co(III)-oxacyclen catalyst **1** (25.2 kcal mol^{-1}) is in better agreement with the values derived from experimental rate constants (25-26 kcal mol^{-1}) than previous mechanistic proposal (~40 kcal mol^{-1}). Within this mechanism, the activity of the process is determined by the energy associated to the nucleophilic attack for Co(III) catalyst, while for Cu(II) the transition state for the final C-N cleavage is isoenergetic with that for nucleophilic attack.

Upon replacing N atoms from the cryptand by less basic O atoms, the Lewis acidity of the metal is enhanced, reducing the overall free energy barrier from 28.5 kcal mol^{-1} for the [N_4] cyclen ligand to 15.2 kcal mol^{-1} for the all-oxygen substituted 12-crown-4 ligand. The assessment of the influence of the nature of the metal ion, reveals that Cu(II) is more reactive than Co(III) due to the larger Brönsted basicity of the Cu-hydroxo moiety. Both trends are in agreement with experimental observations and indicate that Co(III)- and Cu(II)-oxacyclen catalysts play a double role in peptide hydrolysis acting as Lewis acids and Brönsted bases.

COMPUTATIONAL DETAILS

DFT calculations were performed at B3LYP level[49] using Gaussian 09 rev. A02 software.[50] Co and Cu atoms were described by LANL2DZ pseudopotential[51] and Pople's type 6-31G basis set[52] was used for the remaining atoms. Those directly bonded to the transition metal or taking part in reactivity were supplemented with polarization functions to s- and p-type orbitals (referred as B3LYP/DZVP level). Additionally, we have also tested the use of larger basis sets and the addition of dispersion corrections to DFT method on the key steps of the reaction. The geometries were re-optimized using a triple-ζ basis set LANL2TZ[53] supplemented with a f shell[54] for Co and Cu atoms, a 6-311++g(d,p) basis set[52] for the rest of atoms, and D3 dispersion corrections to B3lyp functional[55] (referred as B3LYP-D3/TZVP level). Table S1 compares the two computational levels for the key free energy barriers in peptide hydrolysis by catalyst **1**, and for the influence of the ligand and metal nature in the overall free energy barrier (catalysts **1b** and $\mathbf{1}^{\mathbf{Cu}}$, respectively). The results show the same trends for all the analyzed catalytic steps with small energy differences (~2 kcal mol^{-1}) for overall barriers. Thus, the discussion is mainly based on the more affordable B3LYP/DZVP level, what allows straightforward comparison with previous study on peptide hydrolysis by metal-(oxa)cyclen complex,[28] and our own studies on related peptide bond activation by Zr-substituted polyoxometalates.[43b] To compare computed and experimental results, we make use of Transition State Theory (TST), Eyring equation, in order to estimated free-energy barriers from experimental rate constants (see Table S2 for description of experimental conditions in kinetic studies).

Solvent effects of water were included using the IEF-PCM model[56] as implemented in Gaussian 09. All the species were fully optimized without any symmetry restriction. In addition, all the minima were characterized by the absence of imaginary frequencies and saddle points had a single imaginary frequency associated to the normal mode connecting the corresponding intermediates. For transition states we found **similar** structures to those reported in previous computational studies. All the paramagnetic Cu(II) complexes were computed in the doublet spin state. Gibbs free energies obtained from Gaussian at 298.15 K and 1 atm were corrected using the Whiteside's correction to the translational entropy,[57] following the procedure adapted by Sakaki et al.[58] In this approach we used a water density of 0.997044 $g \cdot cm^{-3}$,[59] and a molecular volume for water of 25.8×10^{-24} cm^3 per molecule.[60] Further discussion about this correction, including the employed equations can be found in the Supporting Information. The results of Whitesides' approach were also compared with the standard state correction to the free energy considering water reactant in solvent concentration (55 mol L^{-1}).[61] The natural bond orbital (NBO) method[62] was used to compute atomic charges and to analyze the resultant wave function in terms of optimally chosen localized orbitals, corresponding to a Lewis structure representation of chemical bonding. To corroborate the NBO results other partition schemes were tested,[63] obtaining the same trends (see Table S3).

ASSOCIATED CONTENT

Supporting Information

The Supporting Information is available free of charge on the ACS Publications website.

Detailed explanation of the employed corrections to Gibbs free energies, additional 3D-representations of key structures and energy profiles, and Cartesian coordinates of the DFT-optimized geometries (PDF)

AUTHOR INFORMATION

Corresponding Author

Jorge J. Carbó - Department de Química Física i Inorgànica, Universitat Rovira i Virgili, Marcel·lí Domingo 1, 43007 Tarragona, Spain.
E-mail: j.carbo@urv.cat

ORCID

Jorge J. Carbó: 0000-0002-3945-6721
Albert Solé-Daura: 0000-0002-3781-3107
Josep M. Ricart: 0000-0002-2610-5535
Maria Besora: 0000-0002-6656-5827

Present Addresses

† Departament de Química, Universitat Autònoma de Barcelona, 08193 Cerdanyola del Valles, Barcelona (Spain).

Notes

The authors declare no competing financial interest.

ACKNOWLEDGMENT

We thank the Spanish Ministry of Science an Innovation (PGC2018-100780-B-I00), the Generalitat de Catalunya (2017SGR629) and the URV for generous support. G. N. also thanks the Erasmus Mundus IMPAKT Scholarship (grant code IT15DM0093).

ABBREVIATIONS

DFT, density functional theory; B3LYP, Becke, 3-parameter, Lee–Yang– Parr; LANL2DZ, Los Alamos National Laboratory 2-double-z; IEF-PCM, Integral Equation Formalism Polarizable Continuum Model; Aβ, Amyloid-beta.

REFERENCES

(1) Bakhtiar, R.; Siuzdak, G.; Thomas, J. J. Mass Spectrometry in Viral Proteomics. *Acc. Chem. Res*. **2000**, *33*, 179−187.

(2) Lewis, J. K.; Bendahmane, M.; Smith, T. J.; Beachy, R. N.; Siuzdak, G. Identification of viral mutants by mass spectrometry. *Proc. Natl. Acad. Sci. U.S.A.* **1998**, *95*, 8596-8601.

(3) (a) Mocz, G. Vanadate-mediated photocleavage of rabbit skeletal myosin. *Eur. J. Biochem*. **1989**, *179*, 373-378. (b) Greiner, D. P.; Hughes, K. A.; Gunasekera, A. H.; Meares, C. F. Binding of the sigma 70 protein to the core subunits of Escherichia coli RNA polymerase, studied by iron-EDTA protein footprinting. *Proc. Natl. Acad. Sci.* **1996**, *93*, 71-75. (c) Heyduk, T.; Heyduk, E.; Severinov, K.; Tang, H.; Ebright, R. H. Determinants of RNA polymerase alpha subunit for interaction with beta, beta', and sigma subunits: hydroxyl-radical protein footprinting. *Proc. Natl. Acad. Sci.* **1996**, *93*, 10162-10166. (d) Cheng, X.; Shaltiel, S.; Taylor, S. S. Mapping Substrate-Induced Conformational Changes in cAMP-Dependent Protein Kinase by Protein Footprinting. *Biochemistry* **1998**, *37*, 14005-14013. (e) Baichoo, N.; Heyduk, T. Mapping cyclic nucleotide-induced conformational changes in cyclicAMP receptor protein by a protein footprinting technique using different chemical proteases. *Protein Sci.* **1999**, *8*, 518-528. (f) Colland, F.; Fujita, N.; Ishihama, A.; Kolb, A. The interaction between σS, the stationary phase σ factor, and the core enzyme of Escherichia coli RNA polymerase. *Genes Cells* **2002**, *7*, 233-247. (g) Loizos, N. Mapping Protein-Ligand Interactions by Hydroxyl-Radical Protein Footprinting. *Methods in Molecular Biology*. **2004**, *261*, 199-210.

(4) (a) Thorner, J.; Emr, S. D.; Abelson, J. N. Applications of Chimeric Genes and Hybrid Proteins, Part A: Gene Expression and Protein Purification. *in Methods in Enzymology*. **2000**, *328*, 326. (b) Wallace, C. J. A. *Protein Engineering by Semisynthesis*, CRC Press: Boca Raton, 2000.

(5) (a) Jartinger, C. G.; Dyson, P. J. Bioorganometallic chemistry--from teaching paradigms to medicinal applications. *Chem. Soc. Rev.* **2009**, *38*, 391-401. (b) Suh, J. Model studies of metalloenzymes involving metal ions as Lewis acid catalysts. *Acc. Chem. Res*. **1992**, *25*, 273-278 (c) Suh, J.; Yoo, S. H.; Kim, M. G.; Geong, K.; Ahn, J. Y.; Kim, M. S.; Chae, P.; Lee, T. Y.; Lee, J.; Lee, J.; Jang, Y. A.; Ko, E. H. Cleavage agents for soluble oligomers of amyloid beta peptides. *Angew. Chem. Int. Ed*. **2007**, *46*, 7064-7067. (d) Lee, T. Y.; Suh, J. Target-selective peptide-cleaving catalysts as a new paradigm in drug design. *J. Chem. Soc. Rev*. **2009**, *38*, 1949-1957. (e) Meggers, E. Targeting proteins with metal complexes. *Chem. Commun*. **2009**, 1001-1010.

(6) See for instance: (a) Wezynfeld, N. E.; Fraczyk, T.; Bal, W. Metal assisted peptide bond hydrolysis: Chemistry, biotechnology and toxicological implications. *Coord. Chem. Rev*. **2016**, *327-328*, 166-187. (b) Suh, J. *in Comprehensive Inorganic Chemistry II, Vol. 6*, 2nd ed. (Ed.: J. Reedijk, K. Poeppelmeier), Elsevier, Amsterdam, 2013, 779-803. (c) Grant, K. B.; Kassai, M. Major Advances in the Hydrolysis of Peptides and Proteins by Metal Ions and Complexes. *Curr. Org. Chem.* **2006**, **10**, 1035-1049.

(7) Jeon, J. W.; Son, S. J.; Yoo, C. E.; Hong, I. S.; Song, J. B.; Suh, J. Protein-Cleaving Catalyst Selective for Protein Substrate. *Org. Lett.* **2002**, *5*, 4155-4158.

(8) Jeon, J. W.; Son, S. J.; Yoo, C. E.; Hong, I. S.; Suh, J. Toward Protein-Cleaving Catalytic Drugs: Artificial Protease Selective for Myoglobin. *J. Bioorg. Med. Chem*. **2003**, *11*, 2901-2910.

(9) Chae, P. S.; Kim, M. s.; Jeung, C. S.; Lee, S. D.; Park, H.; Lee, S.; Suh, J. Peptide-Cleaving Catalyst Selective for Peptide Deformylase. *J. Am. Chem. Soc*. **2005**, *127*, 2396−2397.

(10) Yoo, S. H.; Lee, B. J.; Kim, H.; Suh, J. Artificial Metalloprotease with Active Site Comprising Aldehyde Group and Cu(II)Cyclen Complex. *J. Am. Chem. Soc*. **2005**, *127*, 9593-9602.

(11) Kim, M.-s.; Jeon, J. W.; Suh, J. Angiotensin-cleaving catalysts: conversion of N-terminal aspartate to pyruvate through oxidative decarboxylation catalyzed by Co(III)cyclen. *J. Biol. Inorg. Chem.* **2005**, *10*, 364-372.

(12) Suh, J.; Yoo, S. H.; Kim, M. G.; Jeong, K.; Ahn, J. Y.; Kim, M.-s.; Chae, P. S.; Lee, T. Y.; Lee, J.; Lee, J.; Jang, Y. A.; Ko, E. H. Cleavage Agents for Soluble Oligomers of Amyloid β Peptides. *Angew. Chem. Int. Ed.* **2007**, *46*, 7064–7067.

(13) Jang, S. W.; Suh, J. Proteolytic Activity of Cu(II) Complex of 1-Oxa-4,7,10-triazacyclododecane. *Org. Lett.* **2008**, *10*, 481-484.

(14) Suh, J.; Chei, W.; Lee, T.; Kim, M.; Yoo, S.; Jeong, K.; Ahn, J. Cleavage agents for soluble oligomers of human islet amyloid polypeptide. *J. Biol. Inorg. Chem*. **2008**, *13*, 693-701.

(15) Jang, B.; Suh, J. Kinetic Studies on Proteolysis by Co(III) Complex of Cyclen. *J. Bull. Korean Chem. Soc*. **2008**, *29*, 202-204.

(16) Kim, H.; Jang, B.; Cheon, Y.; Suh, M.; Suh, J. Proteolytic activity of Co(III) complex of 1-oxa-4,7,10-triazacyclododecane: a new catalytic center for peptide-cleavage agents. *J. Biol. Inorg. Chem*. **2009**, *14*, 151-157.

(17) Kim, M.; Yoo, S.; Chei, W.; Lee, T.; Kim, H.; Suh, J. Soluble artificial metalloproteases with broad substrate selectivity, high reactivity, and high thermal and chemical stabilities. *J. Biol. Inorg. Chem*. **2010**, *15*, 1023-1031.

(18) Chei, W.; Ju, H.; Suh, J. New chelating ligands for Co(III)-based peptide-cleaving catalysts selective for pathogenic proteins of amyloidosis. *J. Biol. Inorg. Chem*. **2011**, *16*, 511-519.

(19) Kim, M. G.; Kim, H. M.; Suh, J. Artificial Metalloprotease Based on Co(III)oxacyclen-Aldehyde Conjugate. *Bull. Korean Chem. Soc*. **2011**, *32*, 3113-3116.

(20) Suh, J. Progress in Designing Artificial Proteases: A New Therapeutic Option for Amyloid Diseases. *Asian J. Org. Chem*. **2014**, *3*, 18-32.

(21) Jeong, K.; Chung, W. Y.; Kye, Y. S.; Kim, D.; Song, S. Cu(II) Cyclen Cleavage Agent with BTA-derived Binding Group for h-IAPP. *Bull. Korean Chem. Soc*. **2011**, *32*, 1751–1753.

(22) Wu, W.-h.; Lei, P.; Liu, Q.; Hu, J.; Gunn, A. P.; Chen, M.-s.; Rui, Y.-f.; Su, X.-y.; Xie, Z.-p.; Zhao, Y.-F.; Bush, A. I.; Li, Y.-m. Sequestration of Copper from β -Amyloid Promotes Selective Lysis by Cyclen-Hybrid Cleavage Agents. *J. Biol. Chem*. **2008**, *283*, 31657–31664.

(23) Perera-Bobusch, C.; Hormann, J.; Weise, C.; Wedepohl, S.; Dernedde, J.; Kulak, N. Significantly enhanced proteolytic activity of cyclen complexes by monoalkylation. *Dalton Trans*. **2016**, *45*, 10500-10504.

(24) Hu, J.; Yu, Y.-P.; Cui, W.; Fang, C.-L.; Wu, W.-h.; Zhao, Y.-F.; Li, Y.-m. Cyclen-hybrid compound captures copper to protect INS-1cells from islet amyloidpolypeptide cytotoxicity by inhibiting and lysing effects. *Chem. Commun*. **2010**, *46*, 8023–8025.

(25) Jeong, K.; Chung, W. Y.; Kye, Y.-S.; Kim, D. Cu(II) cyclen cleavage agent for human islet amyloid peptide. *Bioorg. Med. Chem*. **2010**, *18*, 2598–2601.

(26) Jeong, K.; Cho, H. R.; Choi, S. H.; Park, Y.; Chae, P. S. Protective effects of cleavage agents on INS-1 cells against h-IAPP-induced apoptosis. *Chem. Commun*. **2012**, *48*, 588–590.

(27) (a) Dobson, C. M. Protein folding and misfolding. *Nature* **2003**, *426*, 884-890; (b) Hardy, J.; Selkoe, D. J. The Amyloid Hypothesis of Alzheimer's Disease: Progress and Problems on the Road to Therapeutics. *Science* **2002**, *297*, 353-356; (c) Selkoe, D. J. Alzheimer's disease: genes, proteins, and therapy. *Physiol. Rev*. **2001**, *81*, 741-766; (d) Selkoe, D. J. Cell biology of protein misfolding: the examples of Alzheimer's and Parkinson's diseases. *Nat. Cell Biol*. **2004**, *6*, 1054-1061; (e) Hamley, I. W. The amyloid beta peptide: a chemist's perspective. Role in Alzheimer's and fibrillization. *Chem. Rev*. **2012**, *12*, 5147–5192.

(28) Zhang, T.; Zhu, X.; Prabhakar, R. Peptide Hydrolysis by Metal-Cyclen Complexes and Their Analogues: Insights from Theoretical Studies. *Organometallics* **2014**, *33*, 1925-1935.

(29) Zhang, T.; Zhu, X.; Prabhakar, R. Mechanistic Insights into Metal (Pd^{2+}, Co^{2+}, and Zn^{2+})−β-Cyclodextrin Catalyzed Peptide Hydrolysis: A QM/MM Approach. *J. Phys. Chem. B*. **2014**, *118*, 4106-4114.

(30) Zhang, T.; Ozbil, M.; Barman, A.; Paul, T. J.; Bora, R. P.; Prabhakar, R. Theoretical Insights into the Functioning of Metallopeptidases and Their Synthetic Analogues. *Acc. Chem. Res*. **2015**, *48*, 192-200.

(31) Pelmenschikov, V.; Blomberg, M. R. A.; Siegbahn, P. E. M. A theoretical study of the mechanism for peptide hydrolysis by thermolysin. *J. Biol. Inorg. Chem*. **2002**, *7*, 284-298.

(32) Bora, R. P.; Barman, A.; Zhu, X.; Ozbil, M.; Prabhakar, R. Which One Among Aspartyl Protease, Metallopeptidase, and Artificial Metallopeptidase is the Most Efficient Catalyst in Peptide Hydrolysis?. *J. Phys. Chem. B*. **2010**, *114*, 10860-10875.

(33) Blumberger, J.; Lamoureux, G.; Klein, M. L. Peptide Hydrolysis in Thermolysin: Ab Initio QM/MM Investigation of the Glu143-Assisted Water Addition Mechanism. *J. Chem. Theory Comput*. **2007**, *3*, 1837-1850.

(34) Brás, N. F.; Fernandes, P. A.; Ramos, M. J. QM/MM Study and MD Simulations on the Hypertension Regulator Angiotensin-Converting Enzyme. *ACS Catal*. **2014**, *4*, 2587-2597.

(35) Díaz, N.; Suárez, D. Peptide Hydrolysis Catalyzed by Matrix Metalloproteinase 2: A Computational Study. *J. Phys. Chem. B* **2008**, *112*, 8412–8424.

(36) Zhu, X.; Barman, A.; Ozbil, M.; Zhang, T.; Li, S.; Prabhakar, R. Mechanism of peptide hydrolysis by co-catalytic metal centers containing leucine aminopeptidase enzyme: a DFT approach. *J. Biol. Inorg. Chem*. **2012**, *17*, 209-222.

(37) Paul, T. J.; Barman, A.; Ozbil, M.; Bora, R. P.; Zhang, T.; Sharma, G.; Hoffmann, Z.; Prabhakar, R. Mechanisms of peptide hydrolysis by aspartyl and metalloproteases. *Phys. Chem. Chem. Phys.* **2016**, *18*, 24790-24801.

(38) Leopoldini, M.; Russo, N.; Toscano, M. Which One among Zn(II), Co(II), Mn(II), and Fe(II) is the Most Efficient Ion for the Methionine Aminopeptidase Catalyzed Reaction?. *J. Am. Chem. Soc*. **2007**, *129*, 7776-7784.

(39) Alberto, M. E.; Leopoldini, M.; Russo, N. Can Human Prolidase Enzyme Use Different Metals for Full Catalytic Activity?. *Inorg. Chem*. **2011**, *50*, 3394-3403.

(40) Suarez, D.; Diaz, N. Molecular Modeling of Bioorganometallic Compounds: Thermodynamic Properties of Molybdocene–Glutathione Complexes and Mechanism of Peptide Hydrolysis. *ChemPhysChem*. **2015**, *16*, 1646-1656.

(41) Ly, H. G. T.; Mihaylov, T.; Absillis, G.; Pierloot, K.; Parac-Vogt, T. N. Reactivity of Dimeric Tetrazirconium(IV) Wells–Dawson Polyoxometalate toward Dipeptide Hydrolysis Studied by a Combined Experimental and Density Functional Theory Approach. *Inorg. Chem*. **2015**, *54*, 11477-11492.

(42) Zhang, T.; Sharma, G.; Paul, T. J.; Hoffmann, Z.; Prabhakar, R. Effects of Ligand Environment in Zr(IV) Assisted Peptide Hydrolysis. *J. Chem. Inf. Model*. **2017**, *57*, 1079-1088.

(43) (a) Jayasinghe-Arachchige, V. M.; Hu, Q.; Sharma, G.; Paul, T. J.; Lundberg, M.; Quinonero, D.; Parac-Vogt, T. N.; Prabhakar, R. Hydrolysis of chemically distinct sites of human serum albumin by polyoxometalate: A hybrid QM/MM (ONIOM) study. *J. Comp. Chem*. **2019**, *40*, 51–61; (b) Solé-Daura, A.; Rodríguez-Fortea, A.; Poblet, J. M.; Robinson, D.; Hirst, J. D.; Carbó, J. J. Origin of selectivity in protein hydrolysis by Zr(IV)-containing metal oxides as artificial proteases. *ACS Catal.* **2020,** *10*, 13455−13467.

(44) Derrik, J. S.; Lee, J.; Lee, S. J. C.; Kim, Y.; Nam, E.; Tak, H.; Kang, J.; Lee, M.; Kim, S. H.; Park, K.; Cho, J.; Lim, M. H. Mechanistic Insights into Tunable Metal-Mediated Hydrolysis of Amyloid-*β* Peptides. *J. Am. Chem. Soc*. **2017**, *139*, 2234-2244.

(45) (a) Solé-Daura, A.; Goovaerts, V.; Stroobants, K.; Absillis, G.; Jiménez-Lozano, P.; Poblet, J. M.; Hirst, J. D.; Parac-Vogt, T. N.; Carbó, J. J. Probing polyoxometalate-protein interactions using molecular dynamics simulations. *Chem. Eur. J.* **2016**, *22*, 15280-15289; (b) Solé-Daura, A.; Poblet, J. M.; Carbó, J. J. Structure–Activity Relationships for the Affinity of Chaotropic Polyoxometalate Anions towards Proteins. *Chem. Eur. J.* **2020**, *26*, 5799-5809.

(46) (a) Jiménez-Lozano, P.; Solé-Daura, A.; Wipff, G.; Poblet, J. M.; Chaumont, A.; Carbó, J. J. Assembly Mechanism of Zr-Containing and Other TM-Containing Polyoxometalates. *Inorg. Chem*. **2017**, *56*, 4148−4156; (b) Maksimchuk, N. V.; Maksimov, G. M.; Evtushok, V. Y.; Ivanchikova, I. D.; Chesalov, Y. A.; Maksimovskaya, R. I.; Kholdeeva, O. A.; Solé-Daura, A.; Poblet, J. M.; Carbó, J. J. Relevance of Protons in Heterolytic Activation of H_2O_2 over Nb(V): Insights from Model Studies on Nb-Substituted Polyoxometalates. *ACS Catal*. **2018**, *8*, 9722−9737; (c) Maksimchuk, N. V.; Ivanchikova, I. D.; Maksimov, G. M.; Eltsov, I. V.; Evtushok, V. Y.; Kholdeeva, O. A.; Lebbie, D.; Errington, R. J.; Solé-Daura, A.; Poblet, J. M.; Carbó, J. J. Why Does Nb(V) Show Higher Heterolytic Pathway Selectivity Than Ti(IV) in Epoxidation with H_2O_2? Answers from Model Studies on Nb- and Ti-Substituted Lindqvist Tungstates. *ACS Catal*. **2019**, *9*, 6262-6275.

(47) Hormann, J.; van der Meer, M.; Sarkar, B.; Kulak, N. From Cyclen to 12-Crown- 4 Copper(II) Complexes: Exchange of Donor Atoms Improves DNA Cleavage Activity. *Eur. J. Inorg. Chem*. **2015**, 4722–4730.

(48) (a) Brown, I. D. What factors determine cation coordination numbers?. Acta Cryst. 1988, B44, 545-553; (b) Gagné, O. C.; Hawthorne, F. C. Empirical Lewis acid strengths for 135 cations bonded to oxygen. *Acta Cryst*. **2017**, *B73*, 956-961.

(49) (a) Becke, A. D. Density-functional thermochemistry. III. The role of exact exchange. *J. Chem. Phys*. **1993**, *98*, 5648-5652; (b) Stephens, P. J.; Devlin, F. J.; Chabalowski, C. F.; Frisch, M. J. Ab Initio Calculation of Vibrational Absorption and Circular Dichroism Spectra Using Density Functional Force Fields. *J. Phys. Chem*. **1994**, *98*, 11623-11627.

(50) Gaussian 09, revision C.01; Gaussian, Inc.: Wallingford CT, **2009**. Frisch, M. J.; Trucks, G. W.; Schlegel, H. B.; Scuseria, G. E.; Robb, M. A.; Cheeseman, J. R.; Scalmani, G.; Barone, V.; Mennucci, B.; Petersson, G. A.; Nakatsuji, H.; Caricato, M.; Li, X.; Hratchian, H. P.; Izmaylov, A. F.; Bloino, J.; Zheng, G.; Sonnenberg, J. L.; Hada, M.; Ehara, M.; Toyota, K.; Fukuda, R.; Hasegawa, J.; Ishida, M.; Nakajima, T.; Honda, Y.; Kitao, O.; Nakai, H.; Vreven, T.; Montgomery, J. A., Jr.; Peralta, J. E.; Ogliaro, F.; Bearpark, M.; Heyd, J. J.; Brothers, E.; Kudin, K. N.; Staroverov, V. N.; Kobayashi, R.; Normand, J.; Raghavachari, K.; Rendell, A.; Burant, J. C.; Iyengar, S. S.; Tomasi, J.; Cossi, M.; Rega, N.; Millam, N. J.; Klene, M.; Knox, J. E.; Cross, J. B.; Bakken, V.; Adamo, C.; Jaramillo, J.; Gomperts, R.; Stratmann, R. E.; Yazyev, O.; Austin, A. J.; Cammi, R.; Pomelli, C.; Ochterski, J. W.; Martin, R. L.; Morokuma, K.; Zakrzewski, V. G.; Voth, G. A.; Salvador, P.; Dannenberg, J. J.; Dapprich, S.; Daniels, A. D.; Farkas, Ö.; Foresman, J. B.; Ortiz, J. V.; Cioslowski, J.; Fox, D. J.

(51) Hay, P. J.; Wadt, W. R. Ab initio effective core potentials for molecular calculations. Potentials for the transition metal atoms Sc to Hg. *J. Chem. Phys*. **1985**, *82*, 270-283.

(52) (a) Francl, M. M.; Pietro, W. J.; Hehre, W. J.; Binkley, J. S.; Gordon, M. S.; Defrees, D. J.; Pople, J. A. Self-consistent molecular orbital methods. XXIII. A polarization-type basis set for second-row elements. *J. Chem. Phys*. **1982**, *77*, 3654-3665; (b) Hehre, W. J.; Ditchfield, R.; Pople, J. A. Self—Consistent Molecular Orbital Methods. XII. Further Extensions of Gaussian—Type Basis Sets for Use in Molecular Orbital Studies of Organic Molecules. *J. Chem. Phys*. **1972**, *56*, 2257-2261; (c) Hariharan, P. C.; Pople, J. A. The influence of polarization functions on molecular orbital hydrogenation energies. *Theor. Chim. Acta*, **1973**, *28*, 213-222.

(53) Roy, L. E., Hay, P. J.; Martin, R. L. Revised Basis Sets for the LANL Effective Core Potentials. *J. Chem. Theory Comput*. **2008**, *4*, 1029–1031.

(54) Ehlers, A. W.; Böhme, M.; Dapprich, S.; Gobbi, A.; Höllwarth, A.; Jonas, V.; Köhler, K. F.; Stegmann, R.; Veldkamp, A.; Frenking, G. A set of f-polarization functions for pseudo-potential basis sets of the transition metals Sc-Cu, Y-Ag and La-Au. *Chem. Phys. Lett*., **1993,** *208*, 111-114.

(55) Grimme, S.; Ehrlich S.; Goerigk, L. Effect of the damping function in dispersion corrected density functional theory. *J. Comp. Chem*. **2011**, *32*, 1456-1465.

(56) Cancès, E.; Mennucci B.; Tomasi, J. A new integral equation formalism for the polarizable continuum model: Theoretical background and applications to isotropic and anisotropic dielectrics. *J. Chem. Phys*. **1997**, *107*, 3032-3041.

(57) Mammen, M.; Shakhnovich, E. I.; Deutch, J. M.; Whitesides, G. M. Estimating the Entropic Cost of Self-Assembly of Multiparticle Hydrogen-Bonded Aggregates Based on the Cyanuric Acid·Melamine Lattice. *J. Org. Chem*. **1998**, *63*, 3821-3830.

(58) Ishikawa, A.; Nakao, Y.; Sato, H.; Sakaki, S. Oxygen Atom Transfer Reactions of Iridium and Osmium Complexes: Theoretical Study of Characteristic Features and Significantly Large Differences Between These Two Complexes. *Inorg. Chem*. **2009**, *48*, 8154-8163.

(59) Hodgman, C. D. *Handbook of Chemistry and Physics* (39th Ed.), Chemical Rubber Publishing, Cleveland, 1957, p. 1993

(60) Perkins, S. J. Protein volumes and hydration effects: The calculations of partial specific volumes, neutron scattering matchpoints and 280-nm absorption coefficients for proteins and glycoproteins from amino acid sequences. *Eur. J. Biochem*. **1986**, *157*, 169-180.

(61) Besora, M.; Vidossich, P.; Lledós, A.; Ujaque, G.; Maseras, F. Calculation of Reaction Free Energies in Solution: A Comparison of Current Approaches. *J. Phys. Chem. A* **2018**, *122*, 1392−1399

(62) Reed, R.; Curtiss, L. A.; Weinhold, F. Intermolecular interactions from a natural bond orbital, donor-acceptor viewpoint *Chem. Rev*. **1988**, *88*, 899–926.

(63) (a) Gross, K. C.; Seybold, P. G.; Hadad, C. M. Comparison of different atomic charge schemes for predicting pKa variations in substituted anilines and phenols. *Int. J. Quan. Chem.* **2002**, *90*, 445-458; (b) Galliot, A.; Gil, A.; Calhorda, M. J. Effects of oxygenation on the intercalation of 1,10-phenanthroline-5,6/4,7-dione between DNA base pairs: a computational study. *Phys. Chem. Chem. Phys.* **2017**, *17*, 16638-16649.

Table of Contents. The revisited mechanism for peptide hydrolysis by Co(III) and Cu(II) complexes with (oxa)cyclen ligands consists of an outer-sphere attack to the amide carbon of a solvent water molecule assisted by the metal-hydroxo moiety. This rationalizes the observed trends: (1) replacing N by O atoms in the ligand accelerates the reaction by increasing the Lewis acidity of the metal, (2) Cu(II) is more reactive than Co(III) complex because the larger Brönsted basicity of the Cu(II)-hydroxo ligand.